Princeton Plasma Physics Laboratory

PPPL- 4980

PPPL- 4980

Response of Impurity Particle Confinement Time External Actuators in QH-mode Plasma on DIII-D

B.A. Grierson, et. al.

JANUARY, 2014

PPPL PRINCETON PLASMA PHYSICS LABORATORY

Prepared for the U.S. Department of Energy under Contract DE-AC02-09CH11466.

Princeton Plasma Physics Laboratory
Report Disclaimers

Full Legal Disclaimer

Trademark Disclaimer

PPPL Report Availability

Princeton Plasma Physics Laboratory:

http://www.pppl.gov/techreports.cfm

Office of Scientific and Technical Information (OSTI):

http://www.osti.gov/bridge

Related Links:

U.S. Department of Energy

Office of Scientific and Technical Information

Fusion Links

Response of Impurity Particle Confinement Time to External Actuators in QH-mode Plasmas on DIII-D

B.A. Grierson[1], K.H. Burrell[2], A.M. Garofalo[2], W.M. Solomon[1], A. Diallo[1], M. O'Mullane[3]

[1] Princeton Plasma Physics Laboratory, Princeton University, Princeton, NJ 08543, USA

[2] General Atomics, P.O. Box 85608, San Diego, CA 92186-5608, USA

[3] Department of Physics, University of Strathclyde, 107 Rottenrow, Glasgow G4 0NG, UK

E-mail: bgriers@pppl.gov

Abstract. A series of quiescent H-mode discharges have been executed with the specific aim of determining the particle confinement time of impurities in the presence of the edge harmonic oscillation. These discharges utilize non-intrinsic, non-recycling fully-stripped fluorine as the diagnostic species monitored by charge-exchange recombination spectroscopy. It is found that the EHO is an efficient means of impurity expulsion from the core plasma, with impurity exhaust rates exceeding those in companion ELMing discharges. As the external torque from neutral beam injection is lowered, the global energy confinement time increases while the impurity confinement time does not display an increase.

Submitted to: *Nucl. Fusion*

1. Introduction

Outward radial transport of low-Z particles such as fusion product helium "ash" and medium to high-Z impurities is essential for maintaining a high fuel-ion ratio and low levels of core contaminating impurities and associated radiation in fusion reactors. Impurity concentrations in the tokamak core during stationary H-mode operation are typically regulated by naturally occurring edge localized modes (ELMs). However, the energy released from ELMs can have significant consequences by decreasing the lifetime of plasma-facing components subject to the large localized heat flux which may be unacceptable in ITER. Quiescent H-mode (QH-mode) is an operational regime maintained without ELMs and with constant density and radiated power that presents and attractive alternative to other ELM-control techniques[1]. Density control in the QH-mode is established by the onset of a benign magnetohydrodynamic (MHD) oscillation with a clear magnetic signature, known as the edge harmonic oscillation (EHO). Radial localization of the EHO has been determined from beam-emission spectroscopy (BES) measurements near the H-mode edge pedestal region encompassing the steep gradient region[2]. In this article we investigate the efficacy of the EHO to expel impurities from the H-mode core. We compare with ELMing conditions, and over a range of controllable parameters such as density, rotation and applied 3D magnetic perturbations known to influence plasma performance.

2. Experimental Technique

Determining particle transport rates of fuel ions and intrinsic impurities is typically complicated by a weak core particle source and poor quantification of the edge particle sources. Fuel ion densities can be controlled by edge gas puffing, centrally deposited neutral beam injection, pellet fueling, divertor configuration, pumping and equilibrium shape control, to name a few. In L-mode plasmas the particle confinement time is short and density is typically maintained by continuous gas fueling. In H-mode plasmas gas

puffing beyond the L-H transition is often not necessary due to the strong wall source and edge recycling. In both cases quantification of the fuel and impurity ion recycling sources are subject to large uncertainties. Therefore particle transport measurements are most easily executed by introduction of particles that are rare to the tokamak environment (non-intrinsic), and on exiting the core plasma, do not re-enter (non-recycling).

By injecting a non-intrinsic, non-recycling impurity and monitoring the uptake and expulsion of the ion from charge-exchange recombination (CER) spectroscopy, the impurity ion confinement time can be revealed by the exponential time-decay of the photoemission after its peak intensity. This simple technique, performed in lieu of an ion density calculation, requires the conditions to be time-stationary during the decay phase of the impurity, as large changes in plasma density can affect the beam stopping. These changes in beam stopping are manifested as changes in charge-exchange emission that does not reflect changes in the density of the introduced impurity ion. The decay time in this study is monitored from central sightlines near the magnetic axis, which is the region of interest for the high fusion reactivity core and the region where high impurity accumulation occurs.

A sequence of QH-mode discharges was executed by varying the plasma density, injected neutral beam torque and applied 3D magnetic field. For all of the experiments reported in this study, a mixture of 90% deuterium and 10% carbon-tetrafluoride was used to introduce fluorine into the tokamak from the valve labeled "GASB" in Fig. 1. The GASB valve has a direct line of sight to the plasma and is not occulted by baffling. Fluorine was chosen due to its unique characteristics. Fluorine is non-intrinsic, and monitoring of the fluorine line emission in discharges prior to deliberately introducing fluorine revealed zero emission. Fluorine is highly reactive and electronegative which minimizes the recycling of this impurity. In each discharge the fluorine emission is negligible prior to the the gas puff, and decays monotonically to noise levels after each gas injection. Fluorine is fully stripped in the core of fusion-grade plasmas with beam-induced charge-echange emission from the F-IX (10-9) transition at 4796 Å, and

complex atomic modeling to determine charge-state ionization balance is unnecessary. An additional $\Delta n = 2$ transition exists for F-IX (13-11) at 4791.6 Å. However, the intensity of this $\Delta n = 2$ feature is weaker than the $\Delta n = 1$ emission intensity and cannot be resolved within the signal-to-noise sensitivity of the system. Additional emission from this $\Delta n = 2$ transition may contribute to a systematic over-prediction of the density of this trace impurity, but this will not bias the purely decaying exponential characteristic of the emission in time-stationary discharges. Gas injection was timed with a 5.0 ms duration gate of approximately 4-6 torr-L/s flow rate to introduce a fluorine level of sufficient intensity for the diagnostics, while minimally perturbing the plasma. An absolute measure of this trace impurity density is presented in Appendix A.

Discharge characteristics for the plasmas in this study are all configured with the toroidal magnetic field oriented in the standard direction for DIII-D with the plasma current in the reverse direction to normal operation, both being clockwise when the tokamak is viewed from above. Reversing the plasma current orients six of the eight neutral beams to inject in the opposite direction to the plasma current. Toroidal rotation quantities are displayed with velocity in machine coordinate toroidal direction, which here is opposite to the plasma current. Ion temperature, rotational velocity and dominant impurity density are measured by CER using the intrinsic fully stripped carbon. Electron density is determined from CO_2 interferometry and Thomson scattering, while electron temperature is measured by Thomson scattering and electron cyclotron emission. The following section displays the photoemission decay during steady conditions for a range of conditions.

3. Impurity Confinement Studies

3.1. Variation with plasma density

As described in in Sec. 2, one simple measure of the confinement time of a trace non-recycling, non-intrinsic impurity is to measure the decay of the emission in a time-

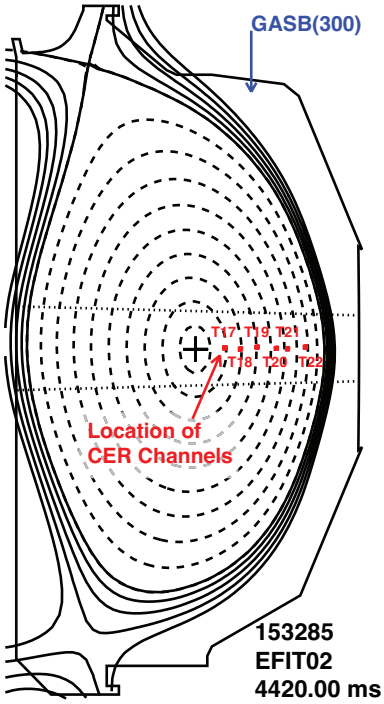

Figure 1. Plasma shape displaying location of gas value and six tangentially viewing CER chords tuned to F-IX(10-9) 4796Å.

stationary plasma. Fig. 2 displays the uptake and expulsion of fluorine measured by a center-most CER viewchord in QH-mode conditions for three different plasma densities. Here the plasma density was first increased by pellet fueling from the high-field side to obtain the intermediate density without triggering ELMs. For the highest density in Fig. 2, the plasma divertor configuration was changed from a strongly cryo-pumping upper-single null to a balanced double null. At low density the emission decay constant is smaller than at high density, indicating that as the plasma density is raised the impurity particle confinement time increases from $\tau_p \approx 350, 450, 600$ ms proportional to the change in electron particle confinement time. Here the analysis is truncated at 5000 ms when the current rampdown begins. Analysis of the fuel particle confinement time from the method in Ref.[3] also indicates a substantial increase in the global electron τ_p with plasma density. Correlation between higher impurity confinement with higher global electron τ_p is consistent with considerations that if the particle transport is determined

by electrostatic turbulence then the transport rate is independent of mass and charge.

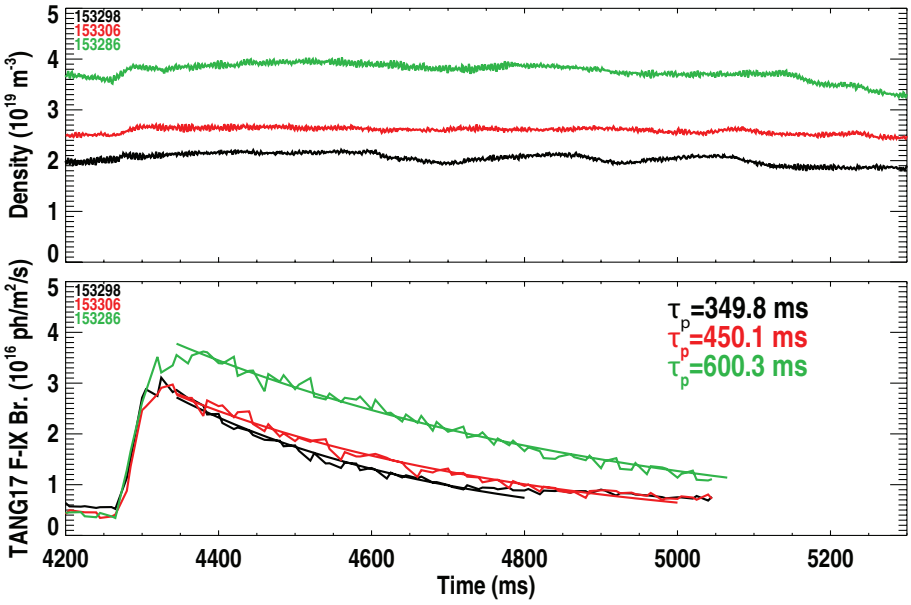

Figure 2. Core emission history of fluorine for three plasma densities displaying an increasing decay constant with increasing density.

3.2. Variation with injected torque and toroidal rotation

The strong scaling of τ_p with plasma density motivates variation of other control quantities with the density held constant. One important control parameter that has clear effects on energy confinement in QH-mode plasmas is the applied NBI torque. QH-mode is a regime where the the energy confinement can be maximized at low NBI torque and low toroidal rotation across much of the plasma minor radius, while maintaining strong $\mathbf{E}\times\mathbf{B}$ rotation shear at the plasma pedestal. The strong edge rotation shear arises either naturally, or with the assistance of non-resonant magnetic field (NRMF) torque through neoclassical toroidal viscosity (NTV)[4]. Therefore a critical question is whether the confinement time of impurities also increases with energy confinement, or if the mechanism for increased energy confinement permits rapid cross-field impurity exhaust while retaining thermal energy. An additional consideration is the effect of applied 3D magnetic perturbations on impurity confinement, as these magnetic perturbations are

used to control the plasma rotation profile. In order to test the particle confinement at low NBI torque, a sequence of discharges was executed at fixed density, while the torque was systematically lowered after the initial startup phase. Fig. 3 displays a torque scan with the plasma density held at $\langle n_e \rangle \approx 2 \times 10^{19}$ m^{-3}. No additional primary gas fueling was required during the torque scan at constant density, which indicates that the global electron τ_p was not increased or decreased as the torque was varied. Torque from NBI was reduced from $T_{inj} \approx$ 4.7N-m to 0.6 N-m, with a corresponding central toroidal velocity decrease from $V_{tor} \approx 310$ km/s to $V_{tor} \approx -20$ km/s. Despite the reduction in toroidal rotation and $\mathbf{E} \times \mathbf{B}$ rotation shear across most of the plasma minor radius, the overall energy confinement increases from $H_{98(y,2)} \approx 0.8$ to $H_{98(y,2)} \approx 1.4$. This increase in confinement is contrary to observations in advanced scenarios[5, 6], which suffer a degradation in confinement as mean $\mathbf{E} \times \mathbf{B}$ shear is reduced by lowering the toroidal rotation. For all discharges in the torque scan, the decay time of the fluorine emission is seen to be approximately constant, with $\tau_p \approx 300 - 400$ ms with no systematic change with torque or rotation. Thus while the energy confinement increases, the particle confinement time does not increase.

3.3. Variation with applied 3D magnetic fields

High-performance, quiescent H-mode plasmas without ELMs have been produced on DIII-D with NBI torque at the ITER-equivalent levels[7, 8]. These plasmas have been maintained with edge rotational shear driven by NTV torque, from NRMF from the 'C-coils' exterior to the DIII-D vacuum vessel. By performing repeat discharges with the same plasma density, but varying the applied 3D magnetic field coil current, effects of the 3D fields on the impurity transport can be determined. Fig. 4 displays the variation in central fluorine emission as the coil current is varied from $0 - 6.0$ kA. The decay constant determined from the fluorine emission is $\approx$ 300-400 ms. It is noteworthy that the zero C-coil current case is dominated by coherent EHO fluctuations and displays a slightly shorter confinement time, while the other cases with applied 3D fields display

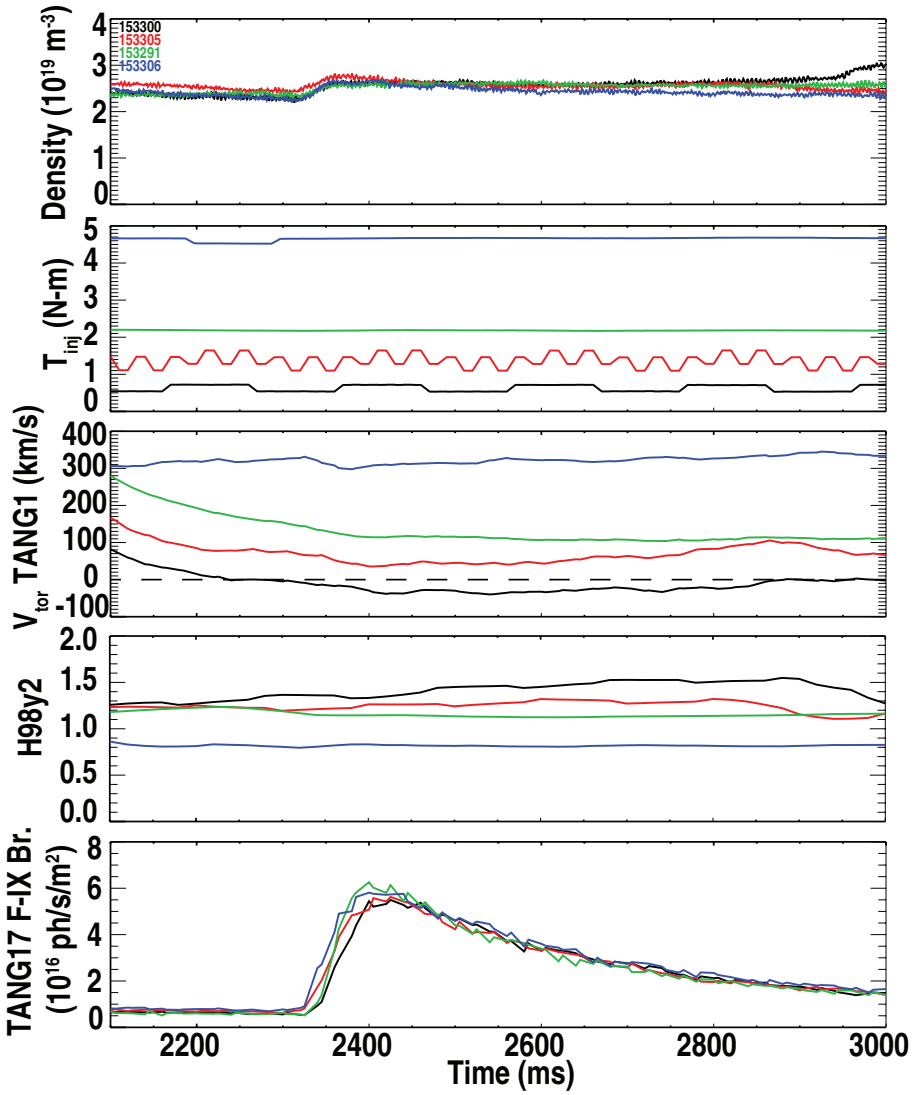

Figure 3. Scan of NBI torque at constant density. Energy confinement increases while impurity confinement τ_p does not increase.

EHO magnetic spectra that are dominantly broadband. Correspondingly the discharge with coherent EHO has a lower pedestal toroidal rotation by approximately 40 km/s, as this mode causes a drag on the wall. Changes in the toroidal rotation profile, EHO mode coherence and applied 3D magnetic perturbation amplitude therefore have a weak effect on the expulsion of impurities in these QH-mode conditions when operating at fixed plasma density.

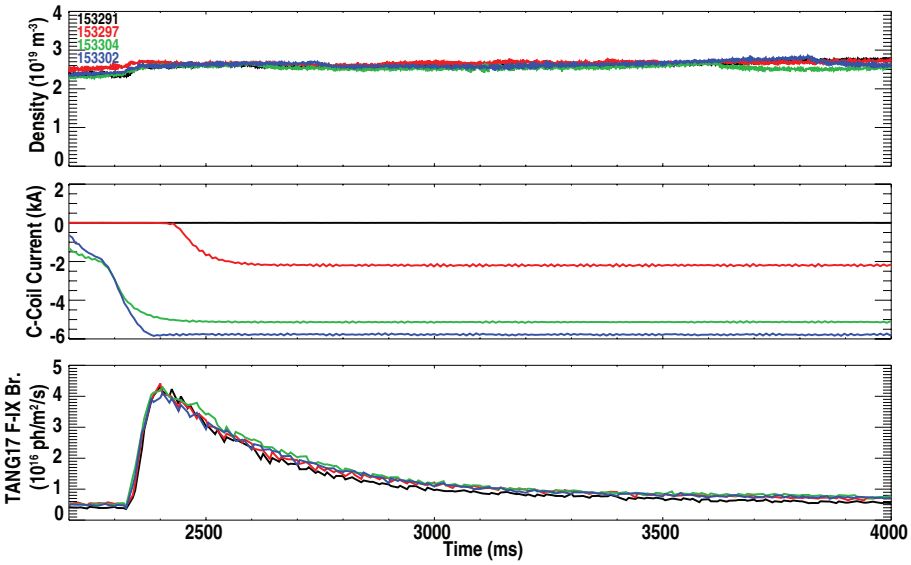

Figure 4. Scan of applied 3D field coil current at constant density. The decay time of the fluorine emission is approximately constant indicating that the applied 3D field has a weak effect on impurity confinement.

3.4. Comparison with ELMing conditions

A critical requirement for any operational scenario with mitigated or absent ELMs is rapid impurity exhaust. In order to assess the impurity expulsion rate induced by the EHO and compare with the impurity expulsion by ELMs, two companion discharges are compared with approximately equal plasma density. In the ELMing discharge the EHO amplitude decays during the early ELM-free phase and disappears, replaced by large ELMs. Fig. 5 displays the time history of the two discharges. Density in the QH-mode is held relatively constant, while the ELMing discharge displays the repeated cycle of density rise and fall during the ELM crash, indicated by the large excursions in the D-alpha time history. Central fluorine emission in these two discharges displayed in Fig. 5(c) decays smoothly for both QH-mode and ELMing conditions, however it is clear that the decay constant τ_p is smaller in the QH-mode. This displays more rapid expulsion of the impurity by the continuous transport provided by the EHO than the periodic ELMs.

A database of discharges that are QH-mode or ELMing during this experimental

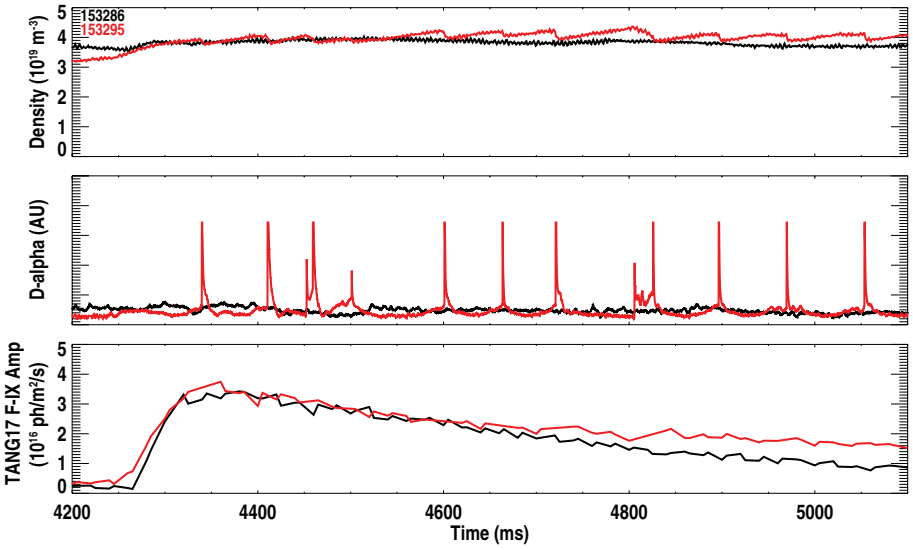

Figure 5. Comparison of QH-mode and ELMing H-mode fluorine confinement demonstrating more rapid expulsion of impurities by the EHO compared to ELMs.

campaign on impurity transport has been compiled to assess the general scaling of impurity confinement time for QH-mode and ELMing discharges during steady periods. Fig. 6 displays the fluorine particle confinement as a function of line averaged density from the CO_2 interferometer. Fluorine impurity confinement scales directly with total plasma density for the QH-mode, while the density scaling of the ELMing conditions in this database is not readily apparent due to the lack of large density variation. As can be seen in Fig. 6, the impurity confinement times are smaller for all QH-modes in this study compared to ELMing conditions.

4. Conclusions

Demonstration of rapid impurity exhaust in discharges with mitigated, triggered and suppressed ELMs is critical for assessing reactor relevance. In this article we have used a non-intrinsic, non-recycling impurity to determine the impurity confinement time of fully stripped fluorine (Z=9) for a range of plasma conditions and external actuators used to control H-mode discharges. We find that the strongest dependence of the impurity confinement appears with a linear relation to global plasma density. Other actuator

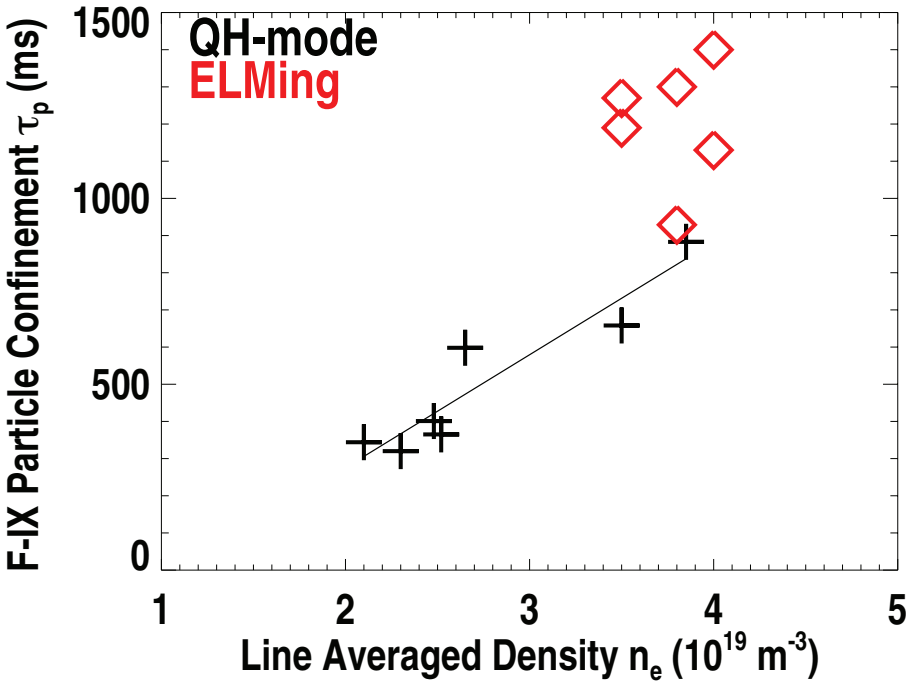

Figure 6. Trends of impurity confinement time as a function of plasma density for QH-mode and ELMing H-mode conditions. QH-mode conditions have more rapid transport of core impurities than ELMing conditions for a range of densities.

scans were therefore executed holding the plasma density fixed. Application of 3D magnetic fields that have been used to access reactor relevant levels of NBI torque are found to modify the mode structure of the EHO, but do not affect the effectiveness of the EHO for transporting particles. At low neutral beam torque and low toroidal rotation, the energy confinement is maximized in the QH-mode, while the impurity confinement does not display any measurable increase. The QH-mode displays a lower impurity confinement time than a comparable ELMing discharge, and we find that this is a general feature revealed from a database of QH and ELMing discharges obtained during this campaign. Impurity confinement characteristics of QH-mode plasmas with an EHO present an attractive option for reactor operation without ELMs.

Appendix A. Fluorine Density Profile and Evolution

Impurity confinement studies described in Sec. 3.1-3.4 have displayed the impurity particle confinement trends across a range of actuators used to control H-mode discharges on DIII-D. Further studies on the fundamental nature of particle transport in these discharges by neoclassical and turbulent transport mechanisms will be pursued in more extensive future studies and require an absolute measure of the fluorine density profile. Here we display calculations of absolute fluorine density using charge-exchange rate coefficients derived under ADAS using general charge-exchange processing ADAS315[9]. Fig. A1 displays the photoemission rate coefficients for charge-exchange from the ground state beam neural ($n = 1$) and the first excited state ($n = 2$). These rate coefficients have been used in the iterative deduction of impurity density profiles from charge-exchange recombination spectroscopy in a self-consistent treatment, including the presence of both carbon and fluorine when computing the beam attenuation. Presented in Fig. A2 are profiles of electron, carbon and fluorine charge densities during the peak of fluorine emission. This profile represents the maximum concentration of fluorine in the discharges presented in this work. It can be seen that the charge density from fluorine is much less than the intrinsic carbon, and is considered a trace impurity. Also displayed in Fig. A2(inset) is the contributions to the effective ion charge Z_{eff} from fluorine ($Z_F^2 n_F/n_e$), carbon ($Z_C^2 n_C/n_e$) and the total plasma Z_{eff} from all ions. The radially averaged $Z_{eff} \approx 2.5$.

Future studies on particle transport will be undertaken and compared to modeling to determine fundamental transport properties of these QH-mode discharges. Profile records such as those displayed in Fig. A3 are obtained with sufficient time resolution to determine the particle diffusion coefficient and pinch velocities. Comparison to theoretical models will permit a physics basis for extrapolation to other conditions such as those expected in ITER.

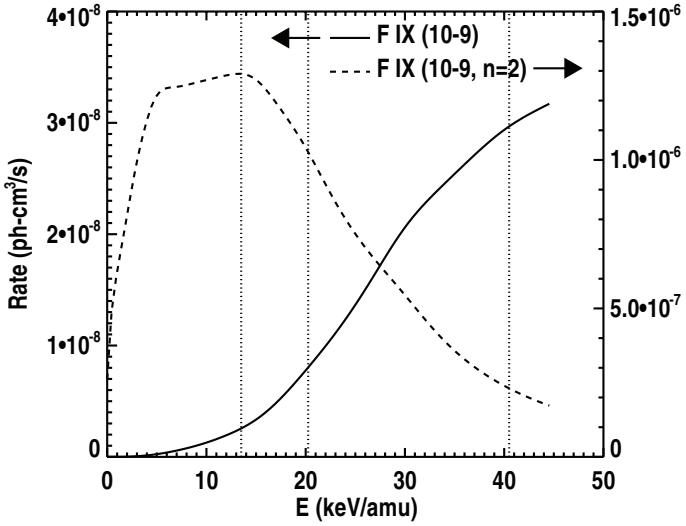

Figure A1. Atomic rate coefficients for fully-stripped fluorine from the ground state and first excited state.

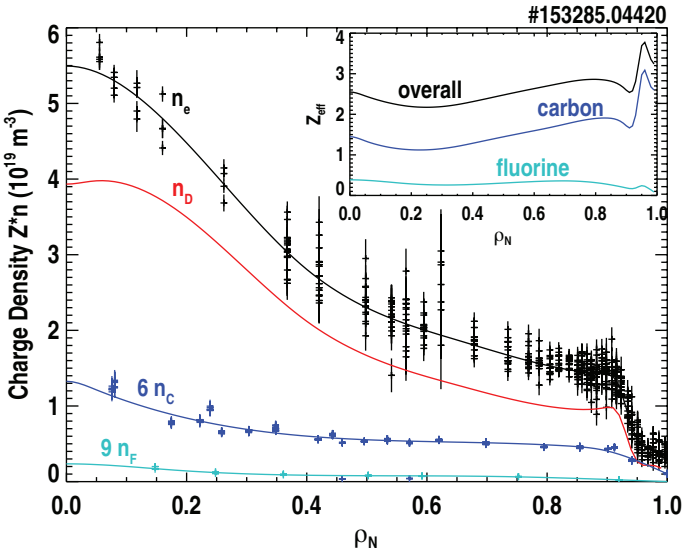

Figure A2. Profiles of measured electron, carbon and fluorine densities as well as deuterium density from quasi-neutrality. Profiles are taken at the peak of central fluorine emission. Impurities are multiplied by their charge. (inset) Contributions to Z_{eff}.

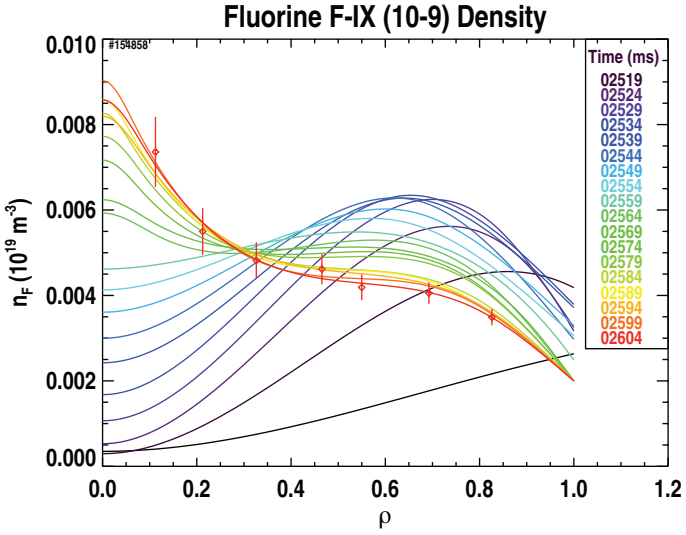

Figure A3. Profiles of the evolution of fluorine density after during a short 5.0 ms gas injection displaying inward propagation of the density from edge to core

Acknowledgments

This work supported in part by the U.S. Department of Energy under DE-AC02-09CH11466 and DE-FC02-04ER54698. The originating developer of ADAS is the JET Joint Undertaking.

References

[1] P T Lang, A Loarte, G Saibene, L R Baylor, M Becoulet, M Cavinato, S Clement-Lorenzo, E Daly, T E Evans, M E Fenstermacher, Y Gribov, L D Horton, C Lowry, Y Martin, O Neubauer, N Oyama, M J Schaffer, D Stork, W Suttrop, P Thomas, M Tran, H R Wilson, A Kavin, and O Schmitz. ELM control strategies and tools: status and potential for ITER. *Nuclear Fusion*, 53(4):043004, March 2013.

[2] K H Burrell, M E Austin, D P Brennan, J C Deboo, E J Doyle, C Fenzi, C Fuchs, P Gohil, C M Greenfield, R J Groebner, L L Lao, T C Luce, M A Makowski, G R Mckee, R A Moyer, C C Petty, M Porkolab, C L Rettig, T L Rhodes, J C Rost, B W Stallard, E J Strait, E J Synakowski, M R Wade, J G Watkins, and W P West. Quiescent double barrier high-confinement mode plasmas in the DIII-D tokamak. *Physics of Plasmas*, 8(5):2153–2162, 2001.

[3] GD Porter. The role of radial particle flow on power balance in DIII-D. *Physics of Plasmas*, 5:4311, 1998.

[4] A M Garofalo, W M Solomon, J K Park, K H Burrell, J C Deboo, M J Lanctot, G R Mckee, H Reimerdes, L Schmitz, M J Schaffer, and P B Snyder. Advances towards QH-mode viability for ELM-stable operation in ITER. *Nuclear Fusion*, 51(8):083018, July 2011.

[5] P Politzer, C Petty, R Jayakumar, T Luce, M Wade, J Deboo, J R Ferron, P Gohil, C T Holcomb, A Hyatt, J Kinsey, R J La Haye, M Makowski, and T Petrie. Influence of toroidal rotation on transport and stability in hybrid scenario plasmas in DIII-D. *Nuclear Fusion*, 48:075001, July 2008.

[6] W M Solomon, P A Politzer, R J Buttery, C T Holcomb, J R Ferron, A M Garofalo, B A Grierson, J M Hanson, Y In, G L Jackson, J E Kinsey, R J La Haye, M J Lanctot, T C Luce, M Okabayashi, C C Petty, F Turco, and A S Welander. Access to high beta advanced inductive plasmas at low injected torque. *Nuclear Fusion*, 53(9):093033, September 2013.

[7] K H Burrell. Reactor-relevant quiescent H-mode operation using torque from non-axisymmetric, non-resonant magnetic fields. *Physics of Plasmas*, 19(5):056117–056117–10, April 2012.

[8] K H Burrell, A M Garofalo, W M Solomon, M E Fenstermacher, D M Orlov, T H Osborne, J K Park, and P B Snyder. Quiescent H-mode operation using torque from non-axisymmetric, non-resonant magnetic fields. *Nuclear Fusion*, 53(7):073038, June 2013.

[9] H P Summers. The adas users manual, version 2.6, 2004. http://www.adas.ac.uk.

The Princeton Plasma Physics Laboratory is operated
by Princeton University under contract
with the U.S. Department of Energy.

Information Services
Princeton Plasma Physics Laboratory
P.O. Box 451
Princeton, NJ 08543

Phone: 609-243-2245
Fax: 609-243-2751
e-mail: pppl_info@pppl.gov
Internet Address: http://www.pppl.gov